

Occurrence of photosynthetic microbial mats in a Lower Cretaceous black shale (central Italy)

A shallow-water deposit

Journal Article**Author(s):**

Pacton, Muriel; Gorin, G.; Fiet, N.

Publication date:

2009

Permanent link:

<https://doi.org/10.3929/ethz-b-000019209>

Rights / license:

[In Copyright - Non-Commercial Use Permitted](#)

Originally published in:

Facies 55(3), <https://doi.org/10.1007/s10347-009-0178-4>

Occurrence of photosynthetic microbial mats in a Lower Cretaceous black shale (central Italy): a shallow-water deposit

Muriel Pacton · G. Gorin · N. Fiet

Received: 22 October 2008 / Accepted: 11 January 2009 / Published online: 7 February 2009
© Springer-Verlag 2009

Abstract Cretaceous oceanic anoxic events (OAEs) were periods of high organic carbon burial corresponding to intervals with excellent organic matter (OM) preservation. This work focuses on the Urbino level, i.e., OAE1b, which is thought to be of regional extent. A detailed microscopical study of OM shows a dominance of microbial activity, characterized by a typical arrangement of exopolymeric substances (EPS) related to microbial mats, bacterial bodies, and some photosynthetic microorganisms, as shown by thylakoids. The latter lived where they have been found, i.e., at the sea bottom, which indicates that OM results from the diagenesis of benthic photosynthetic microbial mats, an interpretation supported through the comparison with a recent analogue. The exceptional preservation of such organic structures in OM points to the joint role of the selective and sorptive preservation pathways. These data and interpretation strongly differ from previous observations in OAE1b equivalents. They suggest that the Urbino level might be an atypical OAE of regional/local extent which was formed within the photic zone.

Keywords Palaeoenvironment · Bacteria · Amorphous organic matter · Extracellular polymeric substances · Sorptive preservation pathway · Oceanic anoxic event

Introduction

Oceanic anoxic events (OAEs) correspond to approximately 50-ka to 1-Ma-long specific intervals of enhanced deposition of organic matter (OM) in marine environments (Schlanger and Jenkyns 1976). They are usually assumed to be deep-water sediments. It is generally accepted that OAEs were associated with major steps in climate evolution, because burial of excess organic carbon must have had an influence on global temperatures by drawing down CO₂. Two models are proposed for the OAE deposition: intense productivity (e.g., Arthur et al. 1985; Pedersen and Calvert 1990; Erba 1994; Weissert et al. 1998; Jenkyns 1999; Premoli Silva et al. 1999; Erba and Tremolada 2004) and a stagnant ocean model arguing for a reduction of deep-water renewal and/or enhanced water column stratification (e.g., Schlanger and Jenkyns 1976; Bralower and Thierstein 1984; Arthur et al. 1990; Tyson 1995; Erbacher et al. 2001). Whereas there are still some uncertainties about the cause(s) of these events, global warmth, increased surface water productivity and/or deep-water stagnation are thought to be intimately associated with them.

OAE1b (Albian) is assumed to have a regional significance. Several expressions of OAE1b are reported in the world, such as in central Italy (Umbria-Marche Basin) where it is called Urbino level (Coccioni et al. 1989), southeastern France (Vocontian Trough), Greece, and ODP legs. In this study, it has been sampled in central Italy, where it does not seem to be affected by metamorphism or hydrothermalism.

The thermohaline stratification hypothesis has been favored for this event, based on $\delta^{18}\text{O}$ values (Erbacher et al. 2001) and planktonic foraminifera (Coccioni et al. 2006) studies. According to these authors, OAE1b is associated with an increase in surface-water temperatures and runoff

M. Pacton (✉) · G. Gorin
Department of Geology-Paleontology,
University of Geneva, 1205 Geneva, Switzerland
e-mail: Muriel.Pacton@unige.ch

N. Fiet
UMR-CNRS 8148, Bat. 504, Paris-Sud University,
91405 Orsay Cedex, France

leading to elevated carbon burial in the restricted basins of the western Tethys and North Atlantic. Hydrocarbon biomarkers data seem to indicate that no unifying mechanism governs the deposition of this black shale interval (Kuypers et al. 2002). The presence of specific biomarkers in equivalent levels (southern France, NW, Greece), i.e., pelagic archaea-derived biomarkers, thought to be the main OM source, reveals a chemotrophic pathway, possibly using ammonium as an energy source (Kuypers et al. 2002; Tsikos et al. 2004).

In this paper, OM sampled in the Urbino level was analyzed using different techniques that include electron microscopy (TEM, SEM) and accessorially, Rock-Eval pyrolysis, gas chromatography-isotope ratio mass spectrometry. The Urbino level in Monte Petrano (see below) and in the Contessa Quarry (Gubbio) is only 20 cm thick. Three samples have been previously studied using Rock-Eval and palynofacies analyses (Fiet 1998). All of them have a total organic carbon content (TOC) considerably higher than 1%, a high hydrogen index ranging from 400 to 620 mgHC/gTOC, $\delta^{13}\text{C}$ values ranging from -22.2 to -25.5% , and show in optical microscopy a similar sedimentary OM constituted essentially of amorphous OM. Consequently, one organic-rich sample has been selected at each of the two locations and can be considered as representative of this thin level.

The main objectives of the study are: (i) to determine the OM composition in the Urbino level (local expression of OAE1b) and (ii) to highlight the processes involved in OM preservation. In order to evaluate the effect of microbial activity, which is commonly considered to be responsible for OM degradation, a recent microbial mat has been used as an analogue. Microbial mats are layered microbial communities usually containing cyanobacteria in the uppermost layers, anoxygenic phototrophic bacteria in intermediate layers (where the mat becomes light-limited) and chemoorganotrophic, especially sulfate-reducing bacteria in the lowermost layers (Konhauser 2007). This comparison is interpreted in terms of microbial/mineral interactions and not from a geochemical point of view.

Materials and methods

Sampling

For a proper comparison of both samples, i.e., the recent microbial mat and fossil OM have been exposed to the same acid treatment and similarly prepared for all analyses carried out.

The studied samples of the Urbino level were collected in Monte Petrano and in the Contessa Quarry (Gubbio) (Marche-Umbria Basin, central Italy; Fig. 1). Sampling was

performed in a 50-cm-deep excavation in order to eliminate surface alteration caused by meteoric waters and vegetation. During transport to the laboratory, sediments were placed in a box sterilized with a bactericidal agent. Potential contamination was tested using DAPI-fluorescence.

The recent microbial mat was sampled in a hypersaline environment at Hassi Jerbi in Southern Tunisia (Davaud and Septfontaine 1995; Fig. 2).

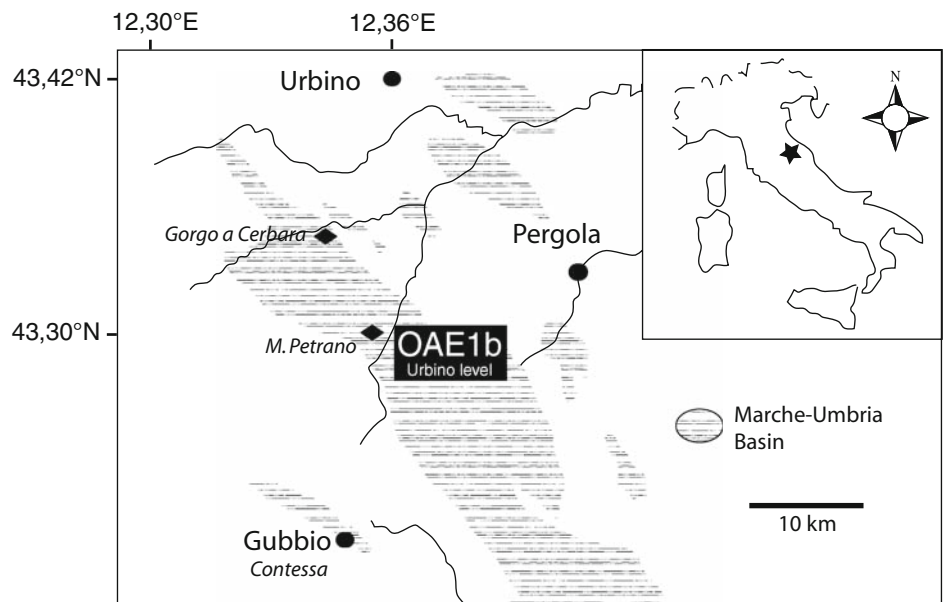
Optical characterization of OM

The observation of fossil OM in consolidated rocks requires a standard palynological preparation technique in order to isolate OM from the mineral fraction. This technique includes HCl and HF acid treatment followed by heavy liquid separation (Steffen and Gorin 1993). The recent microbial mat was exposed to the same acid treatment for a proper comparison with fossil OM. Subsequently, various microscopic techniques were used to analyze the OM morphology and structure down to the nanoscale: optical microscopy (Leitz Diaplan, University of Geneva) using natural light and blue-light fluorescence, scanning electron microscopy (SEM, Jeol JSM 6400, University of Geneva) on gold-coated samples and transmission electron microscopy (TEM) on ultrathin sections. Blue-light fluorescence is an indicator of OM source and also an indicator of the degree of chemical preservation. The fluorescence scale (FS) has been estimated after Tyson (1995). FS1 refers to non-fluorescent OM (matrix and palynomorphs), FS2 is attributed to fluorescent palynomorphs but non-fluorescent matrix, FS3-5 characterized a progressive increase of fluorescent intensity of the AOM matrix and FS6 indicates a strong and homogeneous fluorescence of the AOM matrix. For transmission electron microscopy, bacteria were fixed in 1% glutaraldehyde in 50 mM cacodylate buffer (CB), pH 7.4 at room temperature for 1 h, washed three times in CB, and postfixed in 1% osmium tetroxide in CB for 1 h at room temperature. After washing three times in CB, cells were embedded in 2.5% agarose and dehydrated before inclusion in Epon. Thin sections (70 nm thick) were obtained with a Leica ultramicrotome and contrasted with uranyl acetate. TEM was performed on a Phillips CM100 transmission electron microscope, and digital image processing was applied (Paris-Sud University).

Mineralogy

Mineralogical determinations were performed by standard X-ray diffraction (XRD) on a Philips PW 1729 diffractometer with $\text{CuK}\alpha$ radiation and Ni filter, under 40 kV and an intensity of 25 mA (Paris-Sud University). Analyses were first obtained from bulk rock and secondly from the less than 2- μm -carbonate-free fraction, following the procedure

Fig. 1 Location and stratigraphic column of the Urbino outcrop at Monte Petrano (Marche-Umbria Basin, central Italy)



Epoch	Age	Lithology	Formations	studied organic-rich marker beds
LATE CRETACEOUS	Danian		SCAGLIA ROSSA	
	Maastrichtian			
	Campanian			
	Santonian			
	Coniacian			
	Turonian			
	Cenomanian	SCAGLIA BIANCA		
EARLY CRETACEOUS	Albian		MARNE A FUCOIDI	← Urbino Level (OAE1b)
	Aptian		MAIOLICA	
	Barremian			
	Hauterivian			
	Valanginian			
	Berriasian			
MALM	Tithonian			

100 m

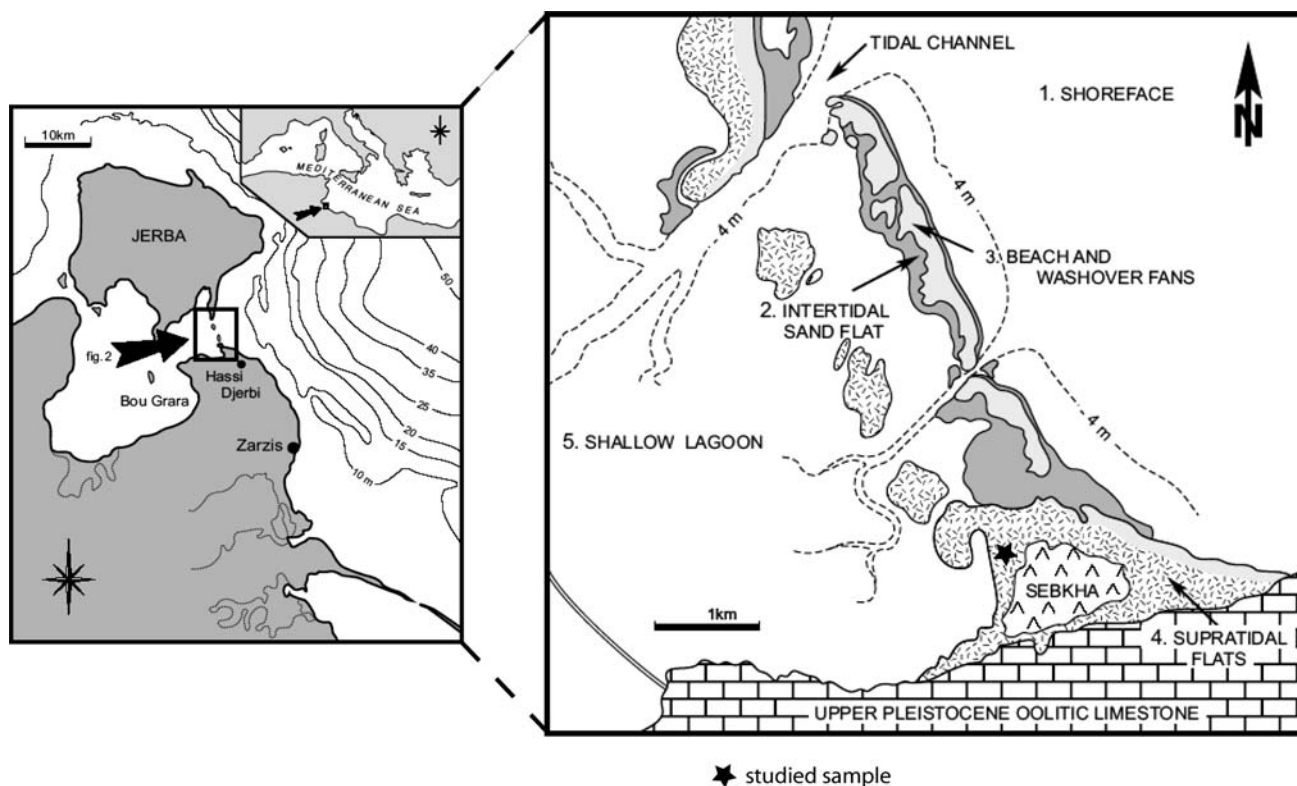


Fig. 2 Geological setting of the Hassi Jerbi outcrop (southern Tunisia)

described by Holtzapfel (1985). Defloculation was carried out through successive washings with distilled water after decarbonation with 0.2 N HCl. Particles smaller than 2 μm were separated by gravitational settling and centrifugation. Three XRD runs were performed on the oriented mounts: (i) untreated; (ii) glycolated (12 h in ethylene glycol); and (iii) heated at 500°C for 2 h. Identification of clay minerals was made according to the position of the (001) series of basal reflections on the three XRD diagrams. Illite, chlorite, kaolinite, smectite, and complex mixed-layers were identified through X-ray diffraction.

Rock Eval pyrolysis

The total organic carbon content (TOC) in the fossil and recent samples was determined using a LECO IR-212 analyzer (Paris VI University). The source and thermal maturity of OM were estimated using a Rock-Eval pyrolysis instrument (Espitalié et al. 1985a, 1985b, 1986). Standard notations are used: S_1 and S_2 are in mg hydrocarbons (HC) per gram of dry sediment and T_{max} is expressed in °C. The hydrogen index ($\text{HI} = S_2/\text{TOC} \times 100$) is expressed in mg HC per gram of TOC.

Carbon and nitrogen isotopes

The kerogen (or insoluble organic matter) was analyzed for carbon and nitrogen isotope composition ($\delta^{13}\text{C}$ and $\delta^{15}\text{N}$)

by flash combustion on an elemental analyzer (Carlo Erba 1108 EA) connected to an isotope ratio mass spectrometer (ThermoFischer/Finnigan MAT Delta S) that was operated in the continuous helium flow via a Conflo II split interface (EA-IRMS). The $\delta^{13}\text{C}$ and $\delta^{15}\text{N}$ values are reported relative to V-PDB and atmospheric nitrogen in air- N_2 (AIR), respectively. The reproducibility, assessed by replicate analyses of laboratory standards was better than 0.1‰ (1 s) for both $\delta^{13}\text{C}$ and $\delta^{15}\text{N}$ values. The accuracy of the analyses was checked periodically by analyses of international reference materials.

Results

Sample characterization

In the Monte Petrano section, the Urbino level appears as a 20-cm-thick, condensed, dark level, made of finely laminated shales (Fig. 3), and intercalated within the “Marne a fucoidi” in the *T. primula*/*H. vischi* ammonite zone (Cocconi et al. 1989; Premoli Silva and Sliter 1994). The recent microbial mat used as an analogue is laminated and composed of an alternation of organic and mineral layers, with a dark, anoxic zone near the surface (Fig. 4).

In fossil OM of the Urbino level, no DAPI-fluorescence has been observed, suggesting that samples have

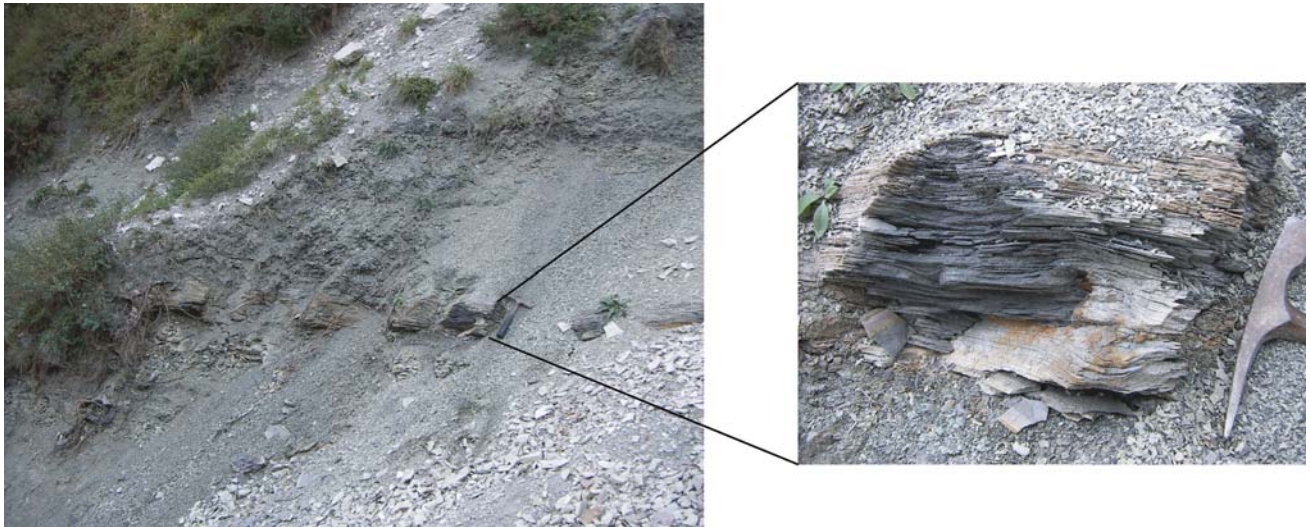


Fig. 3 The Urbino level at Monte Petrano, zoom on the laminated shales



Fig. 4 Cross section of recent microbial mat in the sebkha of Hassi Jerbi (southern Tunisia)

not been contaminated by recent bacteria (sampling, laboratory).

The mineralogy of the Urbino samples differs according to their location. The Monte Petrano sample is made mainly of calcium carbonate (65 wt%) with a detrital part composed of quartz (30 wt%) and clay (5 wt%: illite and montmorillonite), whereas the Contessa sample is mainly siliciclastic with 62 wt% quartz, 13 wt% montmorillonite, 22 wt% illite and 2 wt% kaolinite. The microbial mat is composed of carbonates (24 wt%), halite (16 wt%) and quartz (60 wt%).

In thin section, the Urbino level is characterized by an alternation of parallel organic-rich laminae and mineral lenses (Fig. 5). A rare benthic microfauna has been found. The recent microbial mat is characterized by brown, paral-

lel, organic laminae alternating with heterogeneous intervals, where OM is mixed with quartz grains and few foraminifera (Fig. 6).

Microscopic characterization of OM

In studied fossil samples, no fluorescence has been observed, suggesting an absence of recent contamination (related to laboratory or environmental bacteria). Palynofacies of fossil OM are characterized by dominantly amorphous organic matter (AOM) (85 and 56%, Fig. 7), which appears grumose dark-brown with sharp outlines and patches of heterogeneous size. A minor terrestrial contribution is composed of spores, pollen, and woody

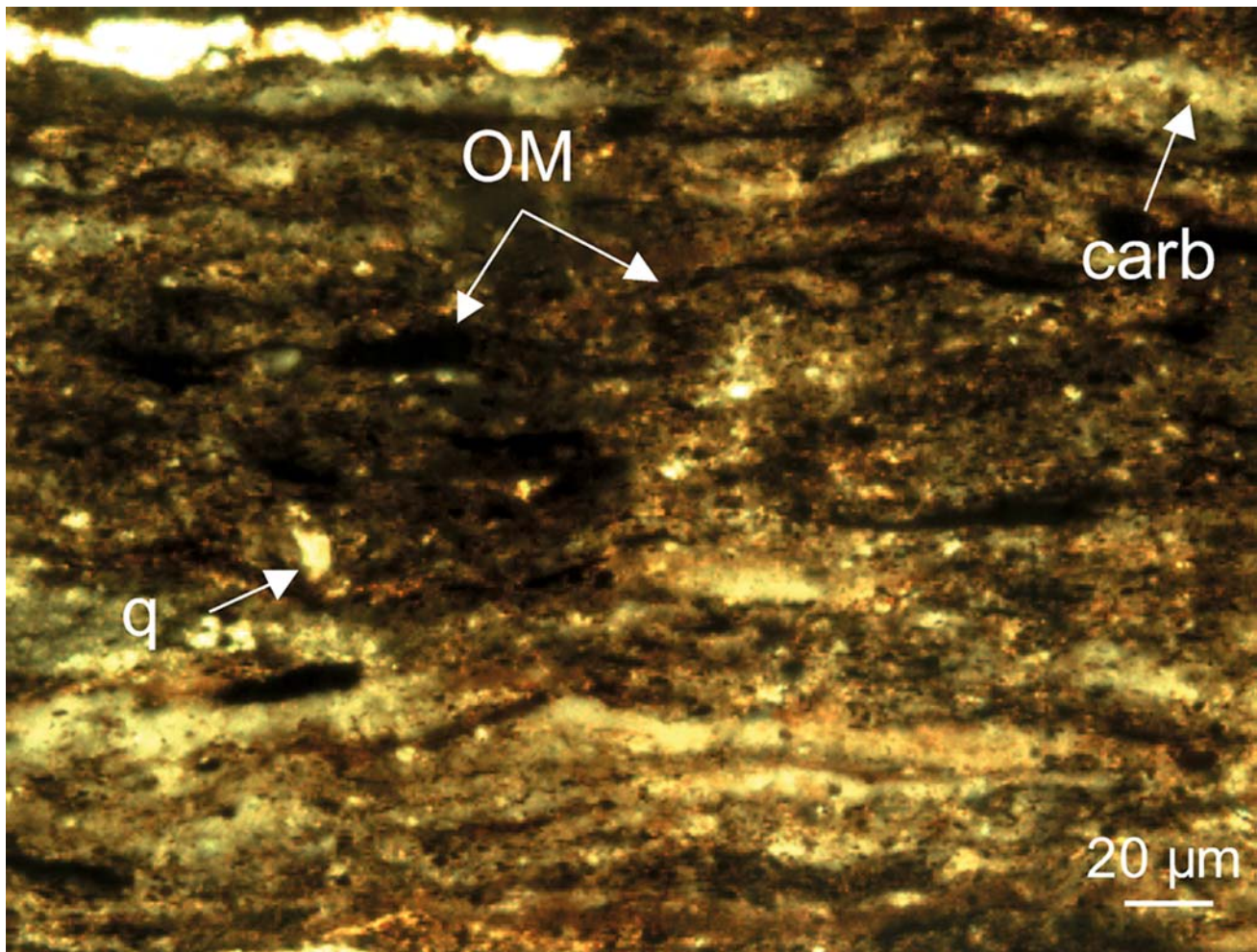


Fig. 5 Petrographic thin section perpendicular to stratification in the Urbino level showing organic-rich laminites with detrital lenses and carbonate grains. *Legend:* organic matter (*OM*), quartz (*q*) and carbonate (*carb*)

fragments. Most of the OM is non-fluorescent, i.e., it has a fluorescence of type FS3 (Tyson 1995, Fig. 8). Some particles show a heterogeneous fluorescence from strong to absent in the Monte Petrano sample, whereas particles are entirely non-fluorescent in the Contessa sample (except for spores and pollen) and correspond to type FS1 (Fig. 9). After undergoing an acid treatment similar to that applied to fossil rocks, the recent microbial mat residue appears mainly composed of AOM and filaments (Fig. 10). An accessory terrestrial contribution is constituted by spores, pollen and dark-brown fibrous vegetal fragments. Filaments are several micrometers long and range from 0.5 to 200 μm in width. Their aspect is translucent to light-brown. AOM appears grumose with sharp outlines and is characterized by a moderate to strong fluorescence, i.e., of type FS4.

In SEM and TEM (Fig. 11), AOM in the Urbino samples is heterogeneous and composed of a widely distributed alveolar network with different orders of magnitude (100 nm to several μm). The same observations can be

made on the recent microbial mat, where elongated structures and an alveolar network are predominant (Fig. 12).

Cocoid cells in fossil OM are characterized by an undulating cell wall with a dark zone inside (Fig. 13a). The same kind of cell has been found in the recent microbial mat where the undulating cell wall is thinner and the dark zone probably represents the cellular content (Fig. 13b). Other types of prokaryotic cells have been identified in fossil OM: microorganism with double-spaced membrane and dark storage inclusions (Fig. 14a); less than 200-nm-wide prokaryote, which is below the size of viable bacteria (Fig. 14b); microbial colonies with a thickened cell wall (Fig. 14c) and exceptionally well-preserved, Gram-negative bacteria containing lipidic inclusions and storage granules (Fig. 14d). The latter bacteria are defined based on the complex cell wall made of two membranes separated by a periplasmic space. The outer membrane is composed of a lipopolysaccharide layer and the periplasmic space separates the plasma membrane from the dark-colored peptidoglycan layer.

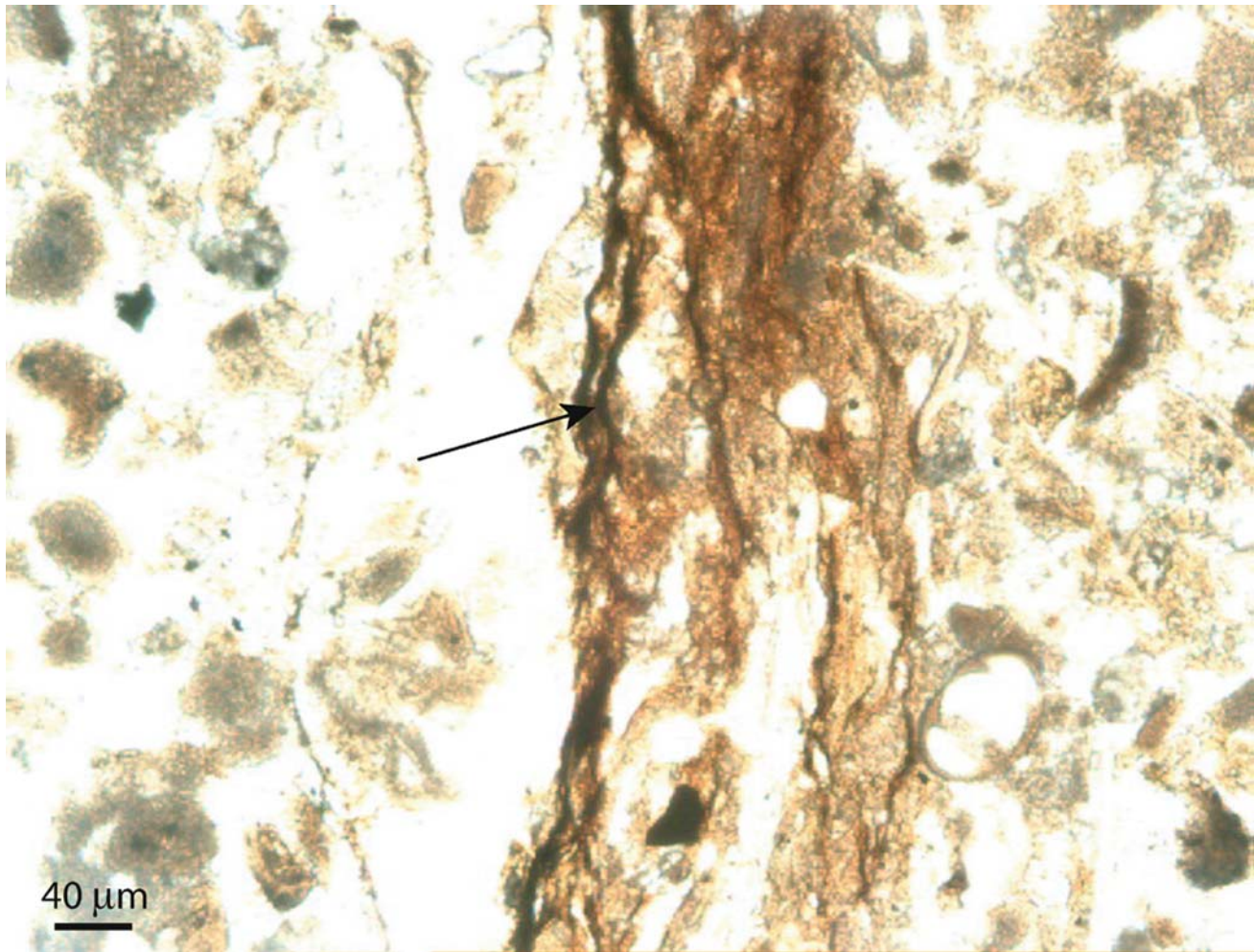


Fig. 6 Petrographic thin section perpendicular to laminations in the recent microbial mat showing organic brown parallel laminae (*black arrow*), organisms and organic clasts

In the fossil OM, numerous occurrences of well-preserved ultralaminae have been found. There are four distinct types of ultralaminae (Pacton et al. 2008): (i) algal cell walls encountered as several μm -large patches, composed of well-defined winding, dense and homogeneous layers up to 150 nm thick (Fig. 15a); (ii) bacterial cell walls appearing as contorted dark filaments with an average thickness of 30–80 nm (Fig. 15b); (iii) thylakoids (membranes where photosynthesis occurs) forming an alternation of dark- and light-colored thin layers with a contorted aspect. They are grouped by pairs bounded by a sharp limit and separated by a diffuse, less contrasted filling (Fig. 15c). Each pair of layers is 20 nm thick, whereas the filling is 50 nm thick; (iv) ultralaminae ascribed to filamentous organisms considering the complexity of the cell wall. They appear as stacked filamentous forms longer than 5 μm and surrounded by a typical layer (Fig. 15d).

In the recent microbial mat, ultralaminae are also dominant and represent algal cell walls which show winding, homogeneous layers with “sharp” outlines and a thickness

ranging from 120 to 180 nm (Fig. 16a). Some 500- to 900-nm-thick, filamentous forms, which are less contrasted (Fig. 16b) than those observed in algal walls, could be ascribed to filamentous bacteria.

Geochemistry

Rock-Eval data for the Urbino sample at Monte Petrano indicate a TOC of 4.3 wt% and a thermally immature type II OM (T_{max} value of 410°C) interpreted as marine (Espitalié et al. 1986). The HI values for fossil and recent OM are identical, i.e., 415 and 416 mgHC/gTOC, respectively. Further characterization of the organic matter was carried out by the isotopic analysis of the kerogen and analysis of the saturated fraction of the extracted bitumen by gas chromatography-mass spectrometry. The carbon and nitrogen isotope composition of the kerogen from the Urbino level ($\delta^{13}\text{C}_{\text{ker}} = -23.8\text{‰}$, $\delta^{15}\text{N}_{\text{ker}} = -1.1\text{‰}$) and of the recent microbial mat ($\delta^{13}\text{C} = -13.2\text{‰}$, $\delta^{15}\text{N} = 2.1\text{‰}$) were measured.

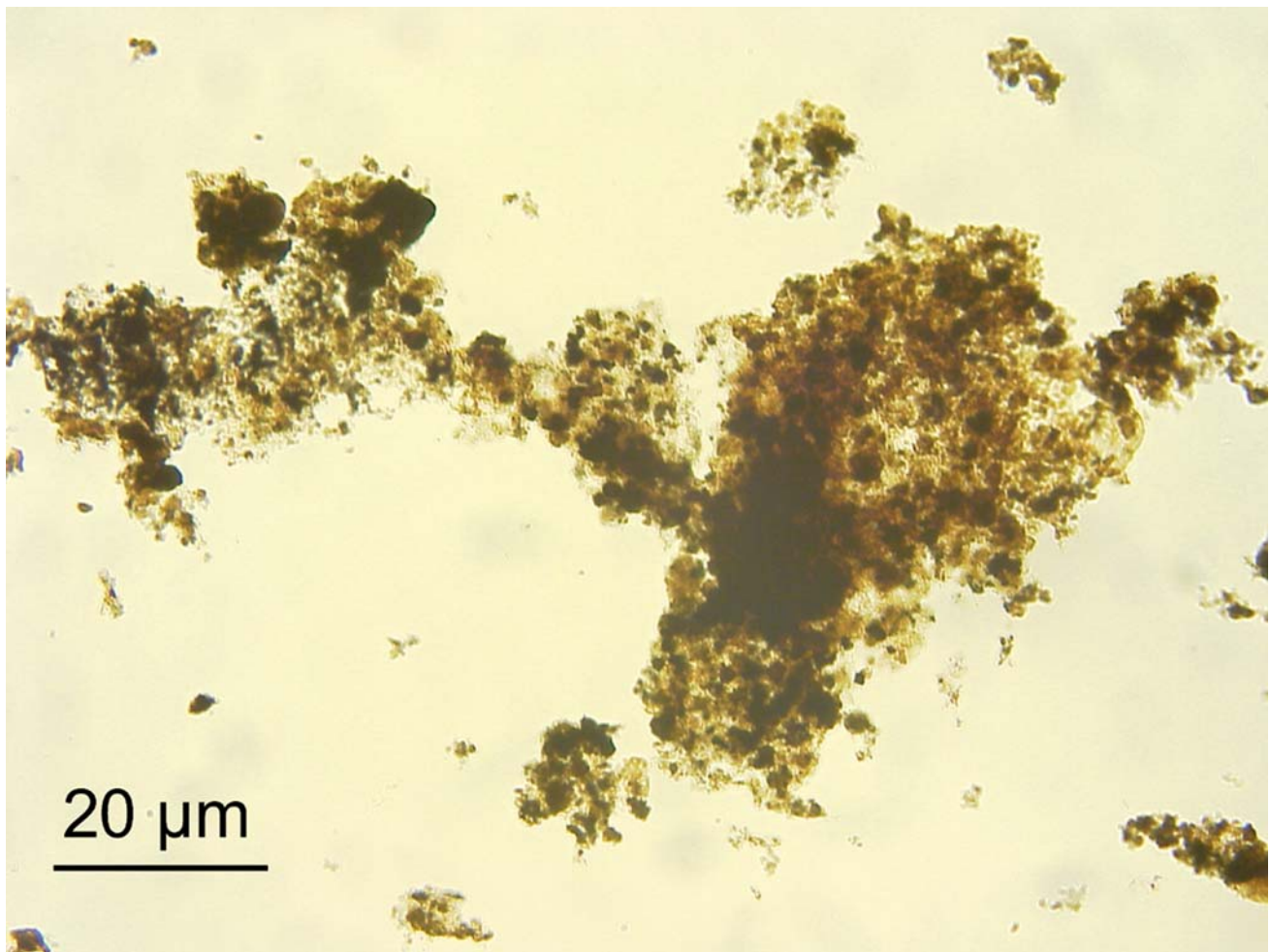


Fig. 7 Palynofacies slide in the Urbino sample: fossil amorphous organic matter (AOM) in transmitted light microscopy

Discussion

Organic matter characterization

Macroscopic observations reveal a laminated alternation of OM and minerals, i.e., laminites, as commonly observed in microbial mats (Fig. 6). Mat development takes place in areas where grazing macrofauna is rare or absent, which is coherent with observations in the Urbino level. Palynofacies in the Urbino level and the recent microbial mat are similar to a dominance of AOM (Figs. 7, 10). The presence of an alveolar network in the OM of both samples (Fig. 11a, b) is indicative of EPS. Previous studies have established that this alveolar network cannot be related to artifacts related to acid treatment or mineral dissolution, but that it is created by mechanical constraints (Pacton et al. 2007). EPS contribute to the fossilization and preservation of OM when they are embedded in microbial mats or biofilms (Pacton et al. 2007). The microscopic observations of EPS, bacteria showing exceptional intact cell walls and internal storage inclusions (Figs. 13, 14), and all types of

ultralaminae, which are generally rarely preserved (Fig. 15), strongly suggest an atypical confined environment with a high physical protection of OM.

$\delta^{13}\text{C}$ values of sedimentary organic matter that are considered to be characteristic of biological CO_2 fixation are based on the assumption that the major CO_2 fixation pathway is that used by cyanobacteria, algae and plants, i.e., the Calvin cycle. Depending on the $\delta^{13}\text{C}$ value of the substrate, sedimentary organic matter with an isotopic signature between -20‰ and -35‰ is usually considered to be Calvin cycle-derived (Schidlowski 1988; Mojzsis et al. 1996). Hoffmann et al. (2000) demonstrated that in late Albian black shales, marine OM is characterized by a $\delta^{13}\text{C}$ value of about -29‰ , whereas terrigenous OM shows values around -23‰ . Therefore, if one applies this observation to the fossil OM in the Urbino level, the $\delta^{13}\text{C}$ value of -23.8‰ would be associated to terrestrial components. However, this is in contradiction with Rock-Eval (type II OM) and palynofacies data (absence of terrestrial constituents), which suggest a bacterial/algal origin.

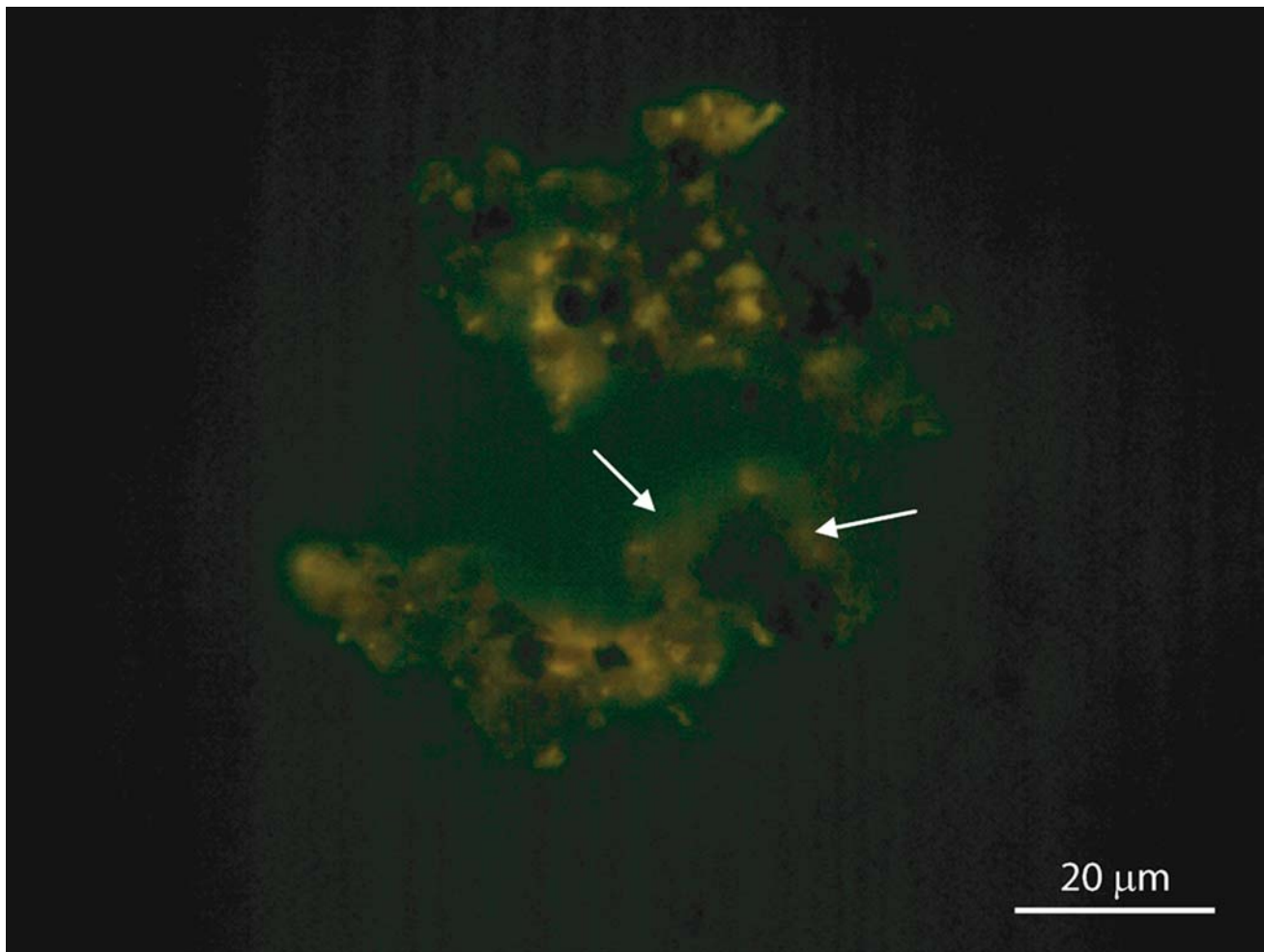


Fig. 8 Palynofacies slide in blue-light fluorescence in the Urbino sample: weakly fluorescent OM from Monte Petrano

In the geological record, carbon isotope signatures of OM that are heavier than that typical of the Calvin cycle might reflect ecologically unique habitats with microorganisms utilizing autotrophic pathways other than the Calvin cycle. Microbial mats in hypersaline systems are sometimes known to have relatively high $\delta^{13}\text{C}$ bulk values of up to -5‰ (e.g., Schidlowski et al. 1984; des Marais et al. 1989; Lazar and Eeres 1992; Kenig et al. 1994; Trichet et al. 2000), which is coherent with that founded in the Hassi Jerbi microbial mat, i.e., -13.2‰ . It has been suggested that the high productivity typically encountered in microbial mats is also responsible for the decreased fractionation of ^{13}C (des Marais et al. 1989; Schidlowski et al. 1994).

The $\delta^{15}\text{N}$ values of recent and fossil samples, close to those of modern atmospheric N_2 ($\delta^{15}\text{N} \approx 0\text{‰}$), suggest a primary contribution of molecular nitrogen fixers, such as photosynthetic cyanobacteria, which have $\delta^{15}\text{N}$ values between -2 and $+4$ per mil (Fogel and Cifuentes 1993). Cyanobacteria function best when the availability of dissolved nitrate is low (Karl et al. 2002), a condition that can be satisfied when ocean water is strongly stratified (Meyers

2006). Therefore, the relatively heavier isotope value of the Urbino level could be explained by microbial rather than terrestrial OM.

Evidence of photosynthetic activity is supported by the presence of cyanobacteria (isotopes) and ultralaminae, i.e., thylakoids (Fig. 15c). The latter are components of phototrophic organisms, which generally constrain water depth to the photic zone (about 200 m) (Mustardy 1996). OM accumulation begins with photosynthesizers at the water surface. In most cases, they are degraded and metabolized throughout the water column. Because thylakoids are highly prone to hydrolysis and physical reactions, their presence supports that photosynthetic/trophic organisms live at the specific depth where thylakoids have been found, i.e., at the sea bottom (Pacton et al. 2008). Their preservation is due to a low degradation thanks to EPS in a complex protected environment, which can be compared to microbial mats.

The comparison of isotopic and microscopic data in terms of microbial/mineral assemblage between the Urbino level and the recent microbial mat supports the interpretation

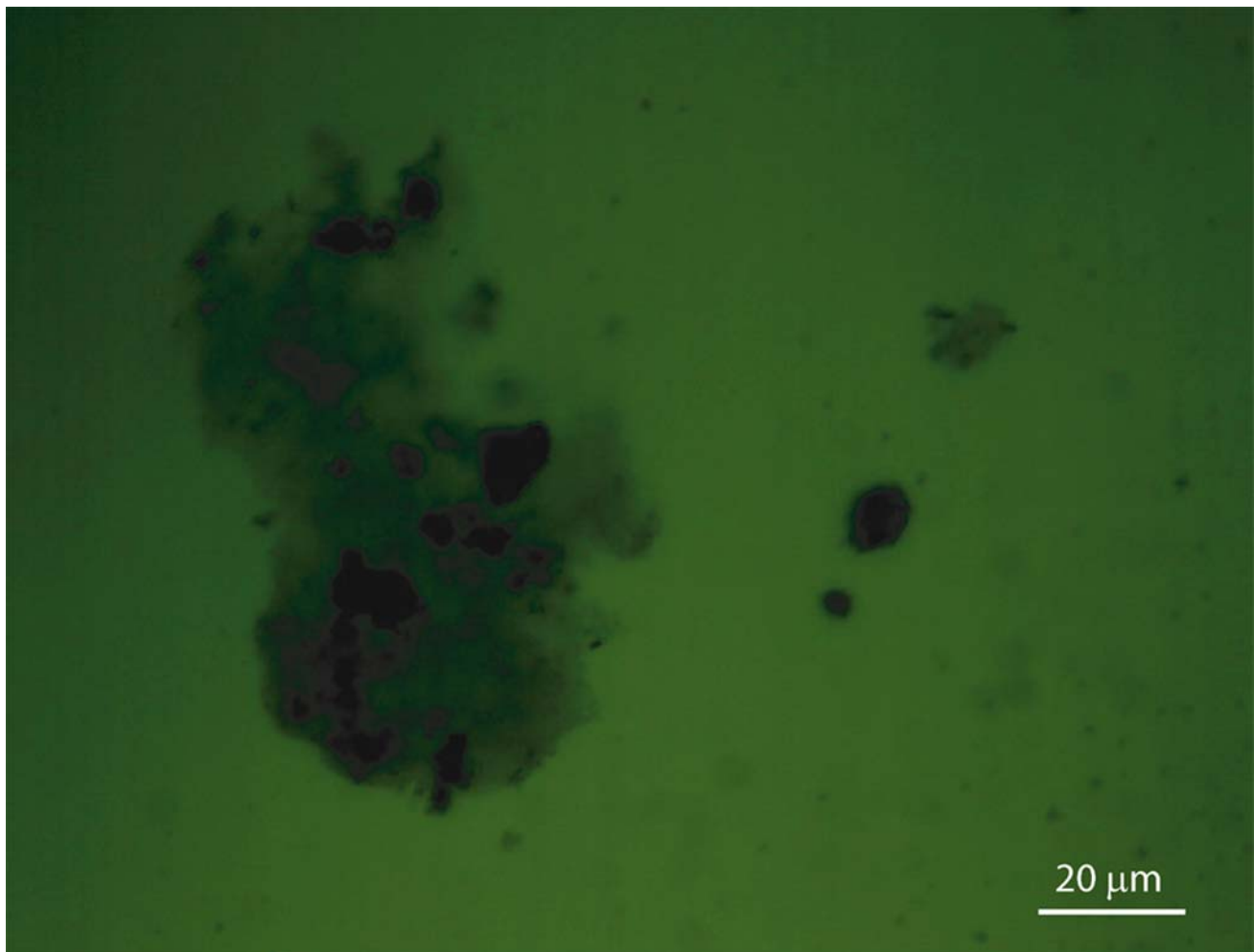


Fig. 9 Palynofacies slide in blue-light fluorescence in the Urbino sample: non-fluorescent OM from Contessa Quarry

that OM in OAE1b is derived from photosynthetic microbial mats. The microbial mat hypothesis in highly dysoxic or anoxic conditions has been used to explain the OM accumulation in OAE1a (leg 198) (Marsaglia 2005). Moreover, benthic microbial mats have been reported in the Selli level (OAE1a) in central Italy (Gorin et al. 2009).

Preservation pathways of organic matter

OM in the Urbino level shows an exceptional degree of preservation (bacteria, ultralaminae). In order to determine which processes are involved in the OM preservation, typical evidence of known preservation pathways has been examined. On one hand, ultralaminae have been shown to originate from the selective preservation of algaenans. The latter are non-hydrolyzable, highly aliphatic macromolecular constituents, which build up very thin (10–30 nm) chemically resistant outer walls in a number of green microalgae (Tegelaar et al. 1989; Derenne et al. 1991). The occurrence of well-preserved ultralaminae in both fossil

OM and recent microbial mat confirms the presence of algae in OM and the role of the selective preservation pathway for OM in the fossil and recently studied samples.

However, the relatively weak fluorescence observed in fossil samples would reflect a strongly degraded material (i.e., reworked by bacteria) or a terrestrial input (Tyson 1995). Nevertheless, not all of the components of the recent microbial mat, which is exclusively composed of recent microbial substances, are fluorescent. This contradicts the standard interpretation (Tyson 1995) and implies that weakly fluorescent AOM does not automatically indicate degraded or terrestrial material, but could also be associated with non-fluorescent EPS. This interpretation is in agreement with the microscopically well-preserved OM as shown by bacteria and ultralaminae encountered in fossil samples.

On the other hand, the sorptive preservation pathway has played a role in the Urbino level as demonstrated by the presence of ultralaminae from bacterial cell walls and thylakoids (Pacton et al. 2008). This is in agreement with EPS present in microbial mats. This sorptive preservation

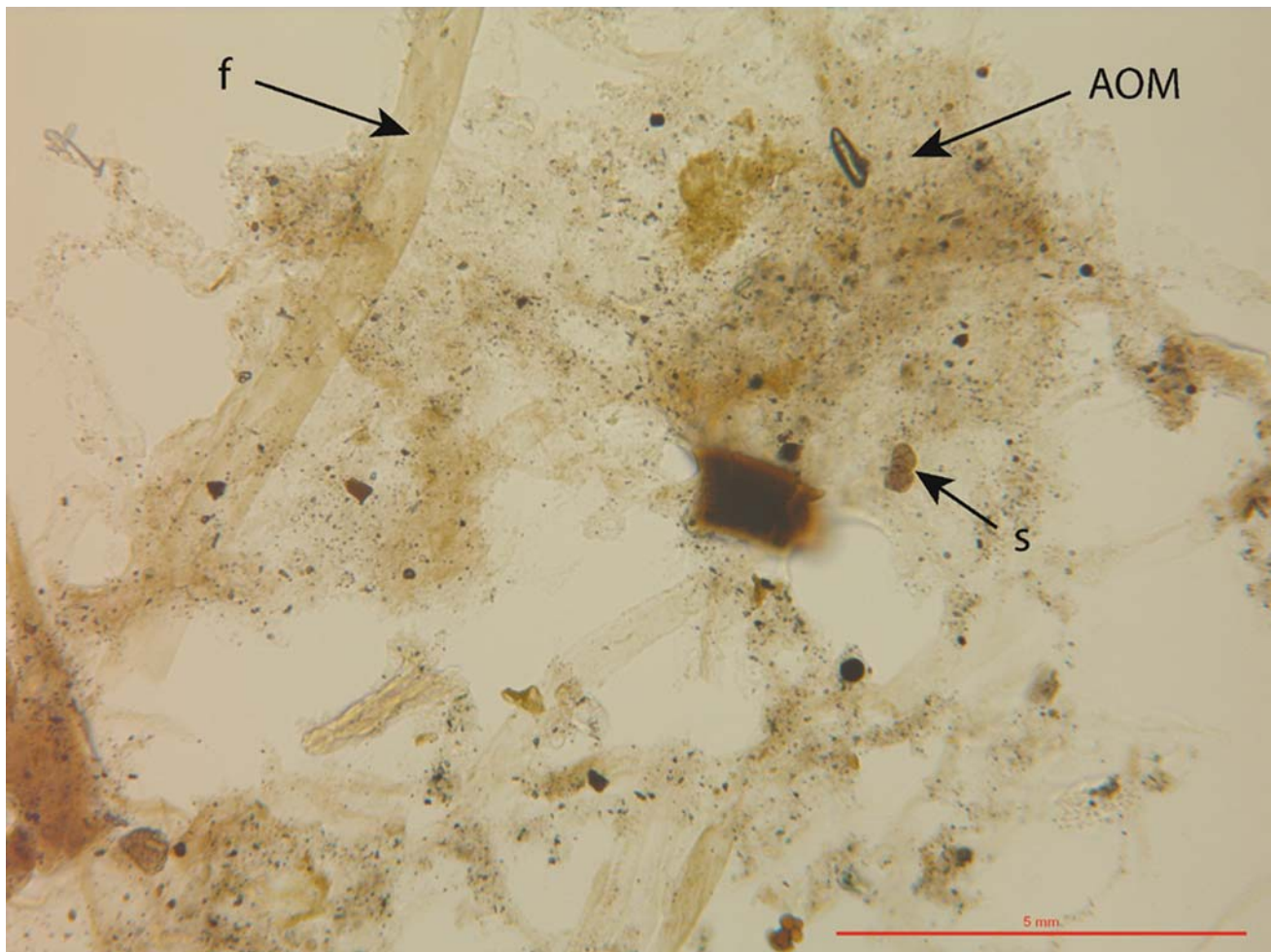


Fig. 10 Palynofacies slide in the recent microbial mat: amorphous organic matter (*AOM*), filaments (*f*) and terrestrial palynomorphs (*s*) in transmitted light microscopy

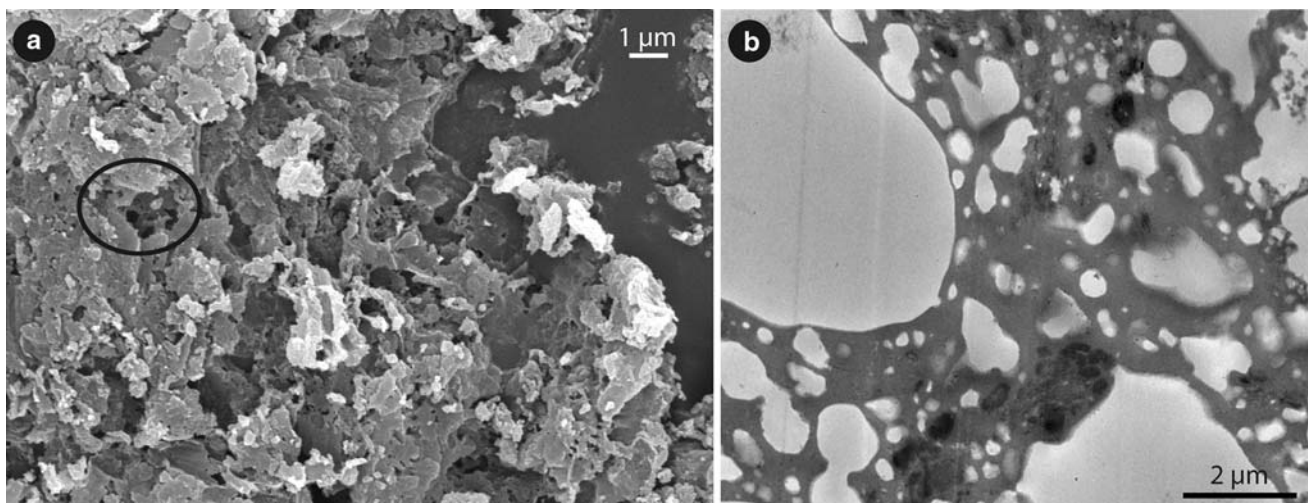


Fig. 11 EPS in fossil OM. **a** SEM showing heterogeneous OM with alveolar network (*circle*). **b** TEM showing alveolar network with different orders of magnitude

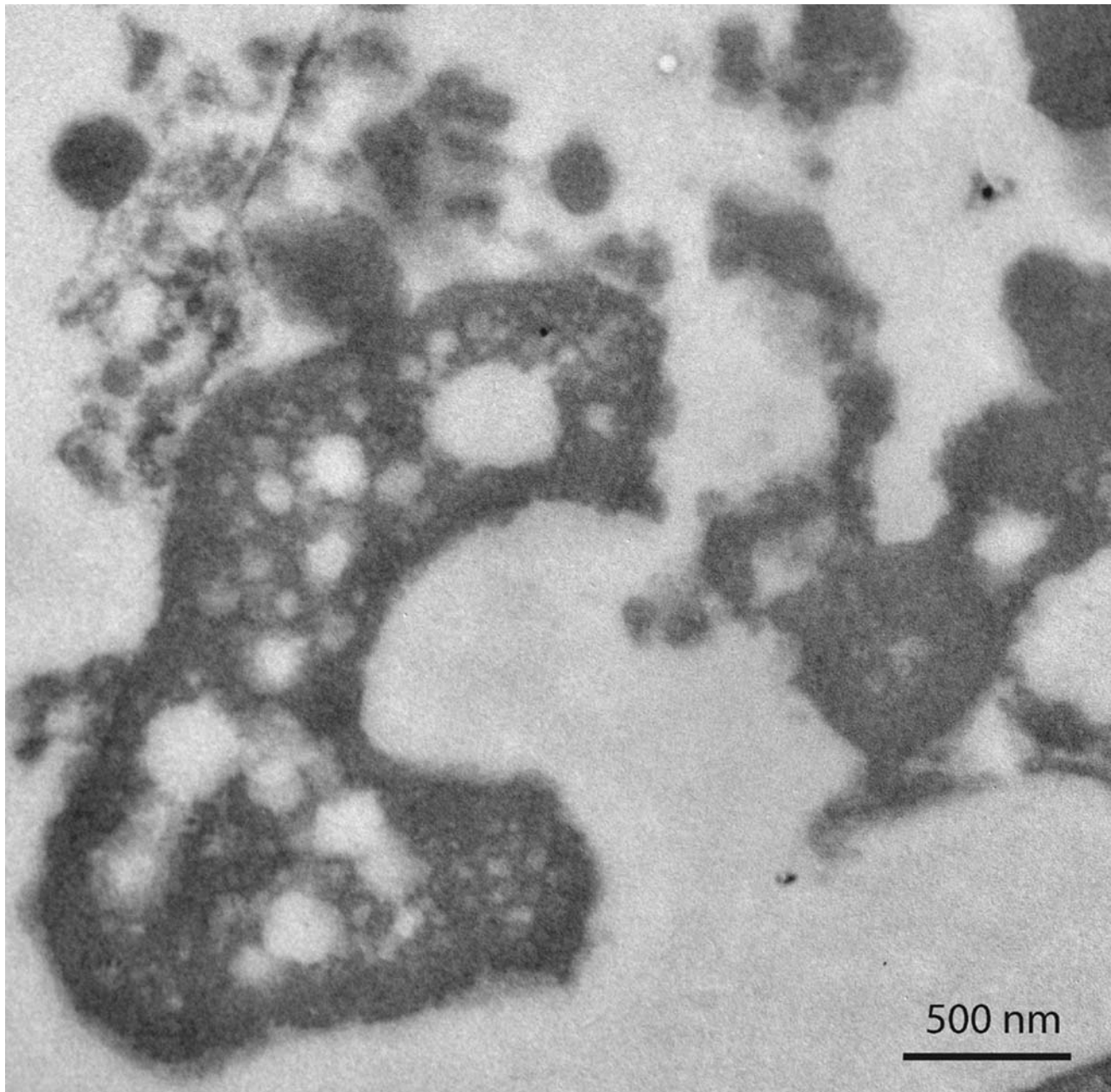


Fig. 12 Ultrathin section of the recent microbial mat in TEM showing alveolar network

is responsible for exceptional OM preservation, not only related to EPS but also to the presence of clays, especially illite and montmorillonite, which are known to play a protective role. In addition to a physical protection from biodegradation (the small size of the pores excludes hydrolytic enzymes), OM adsorption onto pores should favor subsequent condensation reactions by concentrating the reactants (Collins et al. 1995). Salmon et al. (2000) observed that adsorption on the mineral phase possibly played a role, coupled with a physical protection mechanism.

Alternative depositional scenarios

OAEs have so far been identified as deep-water deposits. Therefore, evidence of photosynthetic life for such event at sea bottom is quite controversial. Other possible explanations are envisaged.

Surface photosynthetic productivity

Diazotrophic cyanobacteria have been reported as a primary producer during OAE2 (Ohkouchi et al. 2006). This

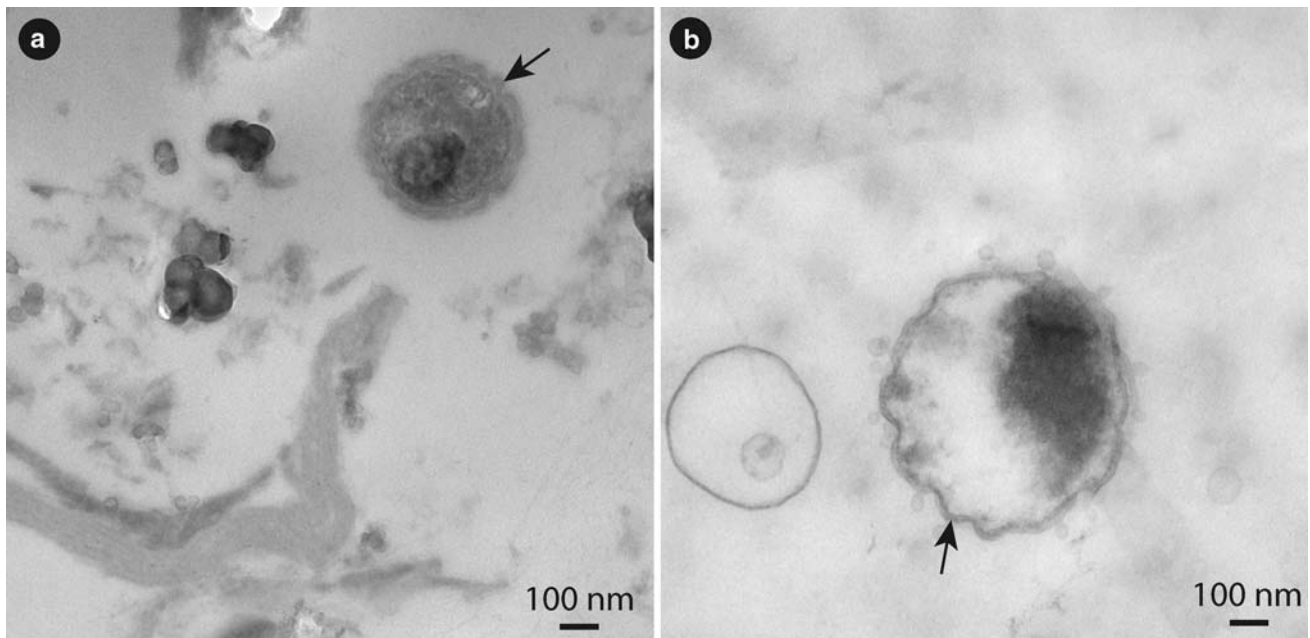


Fig. 13 Ultrathin sections in TEM showing bacterium. **a** In fossil OM, coccoid cell with a thick undulating cell wall and a dark zone inside. **b** In the recent microbial mat, a thin undulating cell wall (*black arrow*) and in dark, the genetic material

supposes warm and oligotrophic surface waters where cyanobacteria lived in the surface oxic layer. This scenario implies that cyanobacteria are metabolized and recycled through the water column. When they sediment, only cell walls escape from complete degradation in reductive environments. This hypothesis does not seem to be compatible with the presence of thylakoids and entire filamentous organisms (i.e., ultralaminae). These would be rapidly degraded during sedimentation through the water column because of their high lability.

Archaea thriving in the marine water column (OM source in the Paquier level)

Typical biomarkers of archaea have been found in an equivalent level, i.e., in southern France (Kuypers et al. 2002) and Greece (Tsikos et al. 2004) and are known in the present-day ocean to be abundant in marine particulate OM and surface sediments (Schouten et al. 2000). The relative contribution of archaeal polymer to the C_{org} can be estimated from $\delta^{13}C_{org}$ by using a two-end-member mixing model: it is assumed that the $\delta^{13}C$ value (approx. -24‰) for bulk sedimentary OM before the OAE1b represents the non-archaeal end-member and $\delta^{13}C = -15.5\text{‰}$ the archaeal end-member (Kuypers et al. 2001). According to these data, $\delta^{13}C$ value in the Urbino level, i.e., approx. -25‰ points to an absence of archaea in the studied OAE1b. However, a close value of -22.1‰ is observed for the sample from OAE1b in Greece, where archaea have been identified from biomarkers. Moreover, halophilic archaea have

been recognized in stromatolites and recent microbial mats (Leuko et al. 2007). Organic geochemistry does not permit a distinction between OM production at the surface or at sea bottom. Therefore, it is possible that archaea lived either in association within the microbial mats, or were thriving in the water column. However, they do not seem to have represented an important component in OM because all microorganisms observed in TEM exhibit a Gram-negative cell wall whereas peptidoglycan is lacking in archaea.

Bacteria living within sapropels

OM in sapropels could still provide a source of carbon and energy for microbial life despite its age (Coolen et al. 2002). For example, Mediterranean sapropels contain prokaryotes, i.e., green non-sulfur bacteria and crenarcheota, which are physiologically active and adapted to these specific palaeoenvironmental conditions because they are abundant in these sediments. Although sapropels are potential energy sources for bacteria over millions of years, they have non-limiting conditions for growth and the organic carbon is recalcitrant, allowing very slow bacterial growth (Parkes et al. 2000). First, if we consider this hypothesis, it is unclear how such ubiquitous EPS could be produced in sediment pore water, and how they could create such a network in the whole OM (with respect to mineral interactions). EPS would appear heterogeneously distributed and the discontinuity would induce a more physical and chemical degradation



Fig. 14 Ultrathin sections in fossil OM in TEM showing different bacteria. **a** Plasma membrane (*p.m.*) and outer membrane (*o.m.*) with dark storage inclusions (*d*). **b** Small bacteria with vacuoles (*v*) (<200 nm in

size); **(c)** in colony; **(d)** Gram-negative (*g.n.*) bacteria with storage (*d*) and lipidic (*l*) inclusions

inhibiting the preservation of bacterial bodies. Moreover, the dominance of microorganisms should be reflected by a strongly fluorescent AOM (FS5 to FS6). This is not the case. Secondly, if observed microorganisms lived after the OM accumulation but before lithification, it implies that the post-OAE1b period would correspond to shallow-water sedimentation because photosynthesis cannot be possible within sediment layers and is limited to 200 m depth.

Comparison to other occurrences of OAE1b

In order to determine the local or regional extent of microbial mats observed in the Urbino level, a comparison has been made with other locations where OAE1b is encountered. Contrary to this study, published papers show mainly organic geochemical and isotopic data, where archaea are thought to be the main OM source. In the Paquier level (OAE1b, southern France) Kuypers et al.

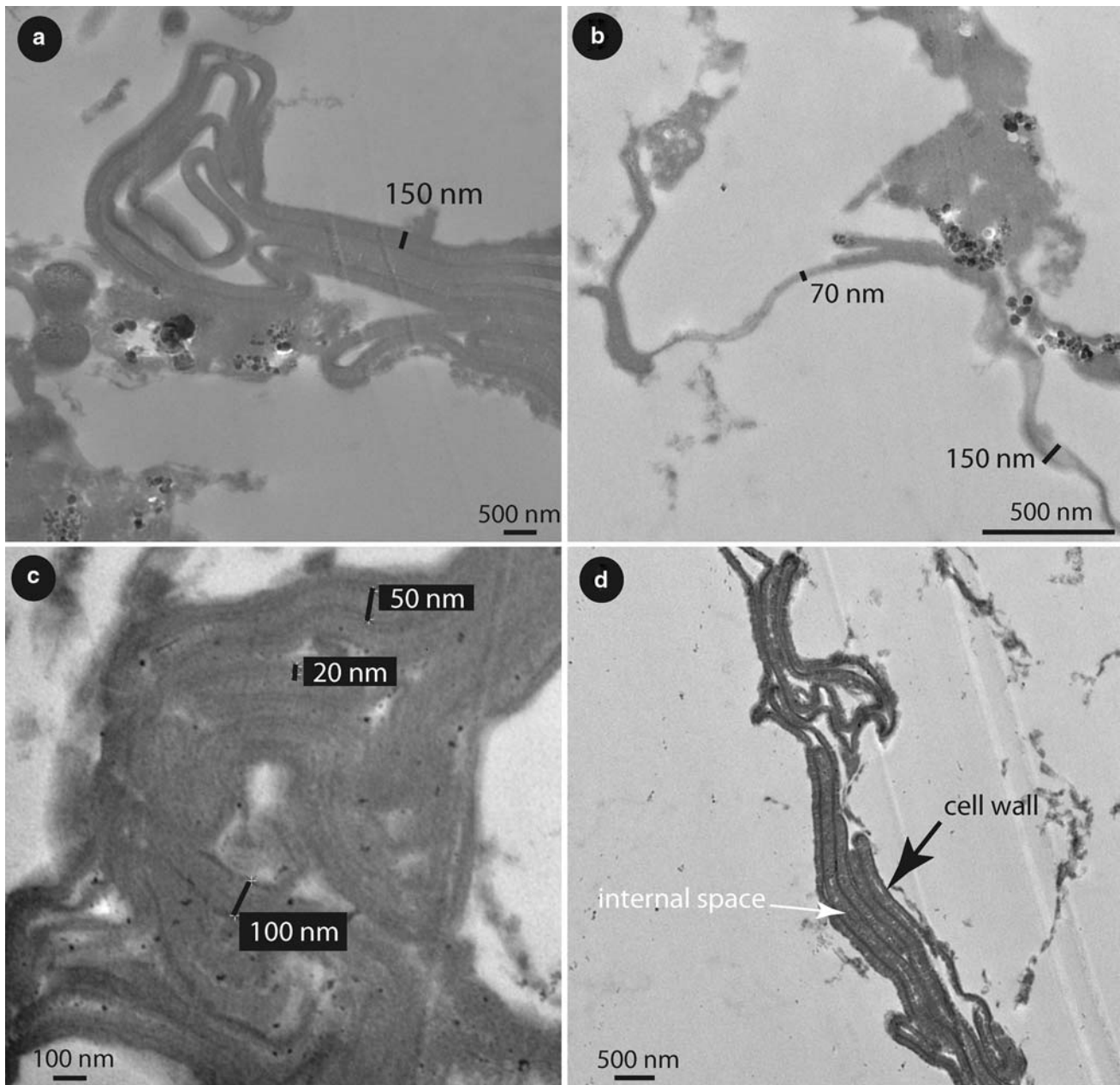


Fig. 15 TEM sections in fossil OM showing **a** algal cell walls patch of contorted layers in the Urbino level, **b** bacterial cell walls: thin contorted layers in the Urbino level, **c** thylakoid membranes contorted pair

of lines in the Urbino level, and **d** filamentous organisms including cell wall and internal filling in the Urbino level

(2001, 2002) characterized microscopically OM as thin laminae of amorphous OM in SEM. Our data present no laminae in SEM but amorphous OM characterized by an alveolar network and other complex components. They display different isotopic data on bulk rock, i.e., a $\delta^{13}\text{C}$ of -15.5‰ , which represents mainly an archaeal source (Kuypers et al. 2001). Data from the Urbino level show a proportion of -25.5‰ . The same authors assumed that the $\delta^{13}\text{C}$ value (approx. -24‰) for bulk sedimentary C_{org} before the OAE1b represents the non-archaeal end-member

and a $\delta^{13}\text{C}$ of -15.5‰ the archaeal end-member (Kuypers et al. 2001). Therefore, $\delta^{13}\text{C}$ values in the Urbino level, i.e., approx. -25‰ point to a weak contribution of archaea in the studied OAE1b. Further studies on biomarkers are required to evaluate the archaea/bacteria proportion in this level.

OAE1b has also been recognized as the uppermost black shale (UBS) in the Ionian Basin (NW Greece, Tsikos et al. 2004). This sample shows a low amount of carbonate (23.3 wt% of CaCO_3 vs. 66% in Monte Petrano), a high-TOC

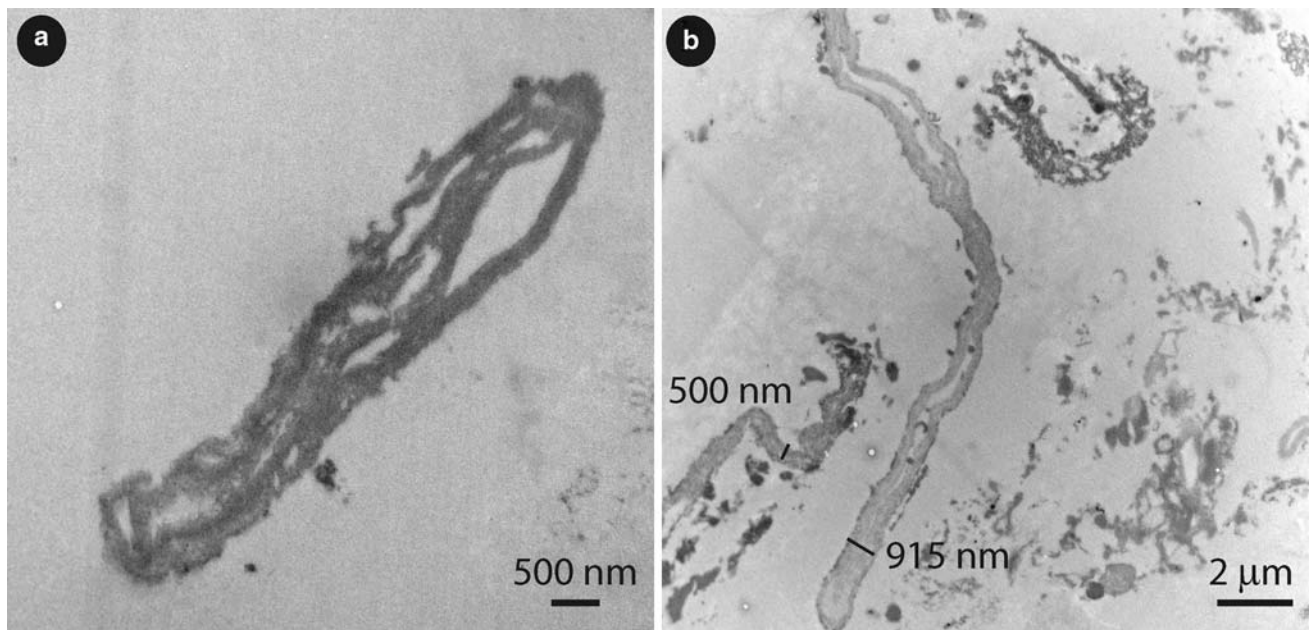


Fig. 16 TEM sections in the recent microbial mat showing **a** algal cell walls, **b** bacterial cell walls dense/translucent fragmented layers in the Hassi Jerbi microbial mat after acid etching; burst translucent

layers attached to dense thin membranes in the Hassi Jerbi microbial mat after acid etching

content, a HI value of 529 mgHC/gTOC (type II, 415 for Monte Petrano) and a $\delta^{13}\text{C}$ of -22.1‰ vs. -25‰ for Monte Petrano. Therefore this sample shows values of $\delta^{13}\text{C}$ and Rock-Eval similar to those in Monte Petrano. However, significant differences are noteworthy in palynofacies analyses: the UBS contains 56% of brightly fluorescence AOM (type 5, Tyson 1995) reflecting a strong algal/bacterial input, whereas the two Urbino samples studied are enriched in non- to poorly fluorescent AOM (56% AOM, FS1 in Contessa and 86% AOM, FS3 in Monte Petrano) characterizing EPS input associated to microbial mats. According to Tsikos et al. (2004), it is debatable whether these data represent a primary isotopic signal or the result of later diagenetic overprinting. They display striking similarities between the UBS in Greece and OAE1b from ODP site 1049C (Kuypers et al. 2002). Therefore, the differences observed in palynofacies data, i.e., AOM quantity and fluorescence (related to the AOM composition), support the local conditions that prevailed during the deposition of the Urbino level.

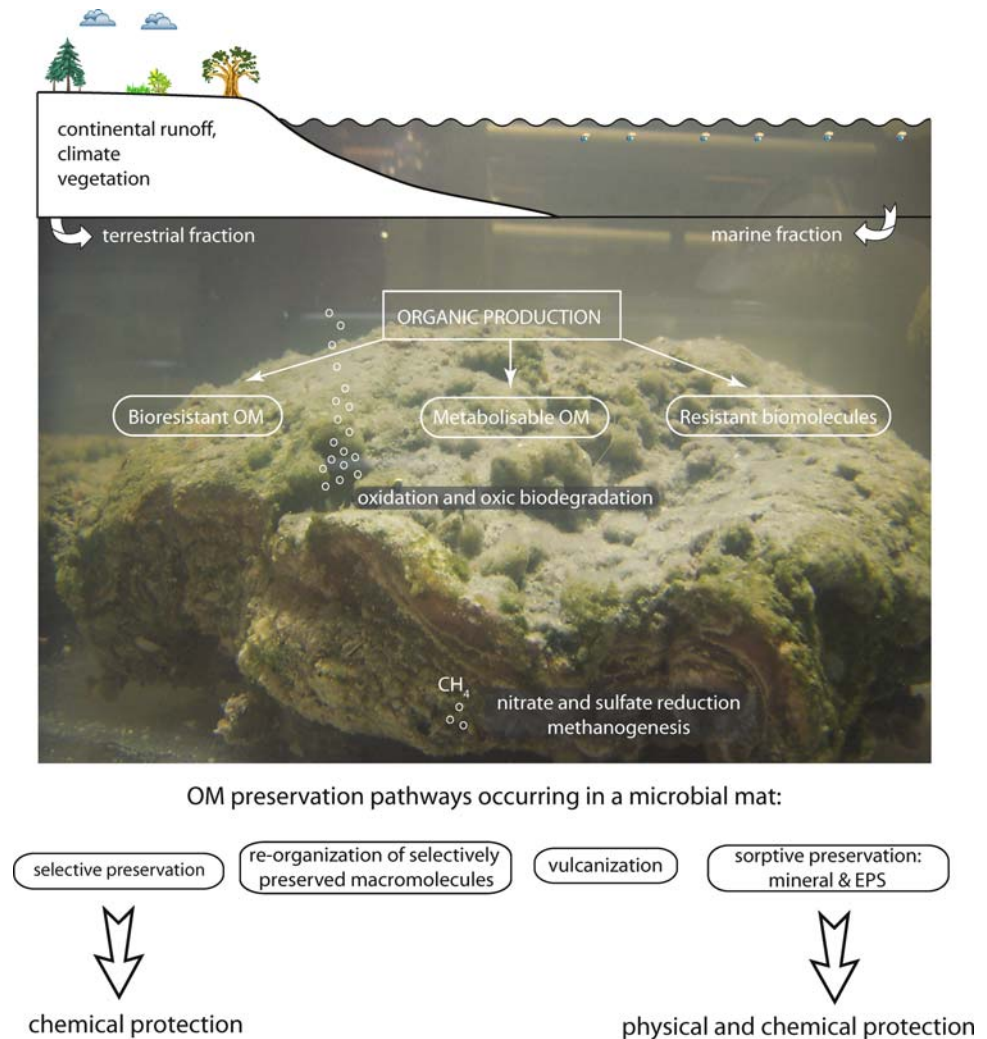
Model of organic matter deposition during the OAE1b

Consequently, we can propose a model of OM deposition during the sedimentation of the Urbino level (Fig. 17). The source of organic and mineral constituents comes from a terrestrial supply of clays, quartz, and palynomorphs, and a marine fraction mainly composed of phytoplankton. The organic accumulation is initiated through biological primary productivity. At sea bottom occurs the development

of benthic photosynthetic microbial mats producing AOM, where cyanobacteria, diatoms, and other microalgae are dominant in the uppermost part of the mat. It becomes slowly enriched in a variety of organic compounds due to the overproduction of carbon during photosynthesis and lysis of the primary producers. Production and preservation of marine OM depend on the composition of phytoplanktonic marine organic tests. Some are enriched in lipidic, bio-resistant macromolecules and labile organic compounds and others are composed of a mineral test and labile OM (Boussafir and Lallier-Vergès 1997). These compounds are degraded by fermentative and heterotrophic bacteria. A mat is governed by complex pathways in which primary production of organic carbon and nitrogen fixation by phototrophy and chemoautotrophy in the upper mat are balanced by heterotrophic decomposition below. Therefore, in a photosynthetic mat where anoxia occurs, nitrate and sulfate reduction and methanogenesis take place thanks to anoxygenic organisms that metabolize cyanobacterial products. The ammonium may be directly utilized by some microorganisms as a nitrogen source, whereas what remains is oxidized to nitrate by nitrifying bacteria (Konhauser 2007).

Selective preservation preserves both morphological and molecular structures: microalgal cell walls (ultralaminariae), dinocysts and terrestrial OM. In the case of bacteria, the preservation process acts so as to re-organize “selectively preserved” molecules. Only the molecular structure is preserved. All organisms produced contribute to the flux of metabolizable OM exported to the sea floor. Organisms

Fig. 17 Model of organic matter deposition during the Urbino level (modified from Boussafir and Lallier-Vergès 1997)



with “organic tests” and bacteria possess naturally bioresistant biomolecules (Boussafir and Lallier-Vergès 1997). The metabolizable OM is generally recycled in the oxic zone. During diagenesis, AOM is greatly protected from chemical and physical degradation by the concomitant presence of EPS and clays through the sorptive preservation pathway. The selective preservation pathway also has an important part in the OM preservation, characterized by the abundance and preservation quality of ultralaminae. The development of such photosynthetic microbial mats points to a possible depositional environment: the Urbino level formed at a water depth within the photic zone.

Conclusions

OM in the Urbino level (OAE1b) is characterized by organic laminites, mainly composed of AOM, with a

minor terrestrial contribution. Microscopic investigations indicate a dominance of microbial activity characterized by EPS, bacterial bodies, and other photosynthetic microorganisms. Based on comparisons with a recent microbial material, sedimentary OM is interpreted to be directly derived from photosynthetic microbial mats. Mechanisms involved in OM preservation are mainly the sorptive preservation pathway (EPS and clay) and the selective preservation pathway.

Consequently, the development of benthic photosynthetic microbial mats implies that this OAE1b in Albian times was formed in relatively shallow water, i.e., within the photic zone. Therefore, this interpretation based on OM sheds a new perspective on OAE research. It challenges the standard interpretation of OAEs, and particularly that of OAE1b (Premoli Silva et al. 1999), confirming that it has a regional extent, but displays locally valid, specific palaeo-environmental conditions.

Acknowledgments This study is supported by the Swiss National Science Foundation (Grants No. 2000.68091 and 2000.112320) and by the UMR-CNRS 8148 I.D.E.S (France), Paris-Sud. The authors thank Jeril Degrouard and Danielle Jaillard (service laboratory for electron microscopy, department of cellular biology, Paris-Sud University, France) for their assistance with TEM imaging and ultramicrotomy. We kindly acknowledge two anonymous reviewers for their highly constructive comments.

References

- Arthur MA, Dean WE, Schlanger SO (1985) Variations in the global carbon cycle during the Cretaceous related to climate, volcanism, and changes in atmospheric CO₂. 2: natural variations Archean to present. In: Sundquist ET, Broecker WS (eds) Chapman conference papers, 1984. The carbon cycle and atmospheric CO, Am Geophys Union; Geophys Monogr 32, pp 504–529
- Arthur MA, Brumsack H-J, Jenkyns HC, Schlanger SO (1990) Stratigraphy, geochemistry, and paleoceanography of organic carbon-rich Cretaceous sequences. In: Ginsburg N, Baudoin B (eds) Cretaceous resources, events and rhythms. Kluwer, Dordrecht, pp 75–119
- Boussafir M, Lallier-Vergès E (1997) Accumulation of organic matter in the Kimmeridge Clay Formation (KCF): an update fossilisation model for marine petroleum source rocks. *Mar Pet Geol* 14:75–83. doi:10.1016/S0264-8172(96)00050-5
- Bralower TJ, Thierstein HR (1984) Low productivity and slow deep-water circulation in mid-Cretaceous oceans. *Geology* 12:614–618. doi:10.1130/0091-7613(1984)12<614:LPASDC>2.0.CO;2
- Coccioni R, Franchi R, Nesci O, Perilli N, Wezel F, Battistini F (1989) Stratigrafia, micropaleontologia e mineralogia delle Marne a Fucoidi (Aptiano inferiore-Albiano superiore) delle sezioni di Poggio le Guaine e del fiume Bosso (Appennino umbro-marchigiano). In: Pallini et al (eds) Fossili, evoluzione, ambiente. Atti del secondo convegno internazionale, Pergola (Italy), 25–30 Ottobre 1987, pp 163–201
- Coccioni R, Luciani V, Marsili A (2006) Cretaceous oceanic anoxic events and radially elongated chambered planktonic foraminifera: paleoecological and paleoceanographic implications. *Palaeogeogr Palaeoclimatol Palaeoecol* 235:66–92. doi:10.1016/j.palaeo.2005.09.024
- Collins MJ, Bishop AN, Farrimond P (1995) Sorption by mineral surfaces: rebirth of the classical condensation pathway for kerogen formation? *Geochim Cosmochim Acta* 59:2387–2391. doi:10.1016/0016-7037(95)00114-F
- Coolen MJL, Cypionka H, Sass AM, Sass H, Overmann J (2002) Ongoing modification of Mediterranean Pleistocene sapropels mediated by prokaryotes. *Science* 296:2407–2410. doi:10.1126/science.1071893
- Davaud E, Septfontaine M (1995) Post-mortem onshore transportation of epiphytic foraminifera: recent example from the Tunisian coastline. *J Sediment Res* A65:136–142
- Derenne S, Largeau C, Casadevall E, Berkaloff C, Rousseau B (1991) Chemical evidence of kerogen formation in source rocks and oil shales via selective preservation of thin resistant outer walls of microalgae: origin of ultralaminae. *Geochim Cosmochim Acta* 55:1041–1050. doi:10.1016/0016-7037(91)90162-X
- des Marais DJ, Cohen Y, Nguyen H, Cheatham M, Cheatman T, Munoz B (1989) Carbon isotopic trends in the hypersaline ponds and microbial mats at Guerrero Negro, Baja California Sur, Mexico: implications for Precambrian stromatolites. In: Cohen Y, Rosenberg E (eds) Microbial mats: physiological ecology of benthic microbial communities. *Am Soc Microbiol*, Wash, DC, pp 191–203
- Erba E (1994) Nannofossils and superplumes: the early Aptian “nannoconid crisis”. *Paleoceanography* 9:483–501. doi:10.1029/94PA00258
- Erba E, Tremolada F (2004) Nannofossil carbonate fluxes during the early Cretaceous: phytoplankton response to nutrification episodes, atmospheric CO₂ and anoxia. *Paleoceanography* 19:PA1008. doi:10.1029/2003PA000884
- Erbacher J, Huber BT, Norris RD, Markey M (2001) Increased thermohaline stratification as a possible cause for an ocean anoxic event in the Cretaceous period. *Nature* 409:325–327. doi:10.1038/35053041
- Espitalié J, Deroo G, Marquis F (1985a) La pyrolyse Rock-Eval et ses applications: Deuxième partie. *Rev Inst Fr Pet* 40:755–784
- Espitalié J, Deroo G, Marquis F (1985b) La pyrolyse Rock-Eval et ses applications: Première partie. *Rev Inst Fr Pet* 40:563–579
- Espitalié J, Deroo G, Marquis F (1986) La pyrolyse Rock-Eval et ses applications: Troisième partie. *Rev Inst Fr Pet* 41:73–89
- Fiet N (1998) Stratigraphie intégrée d’une série pélagique à horizons enrichis en matière organique («black shales»). L’Aptien-Albien du bassin de Marches-Ombrie (Italie centrale). PhD Thesis, Ecole des Mines de Paris—ENSMP, 283 pp
- Fogel ML, Cifuentes LA (1993) Isotope fractionation during primary production. In: Engel MH, Macko SA (eds) Organic geochemistry. Plenum Press, New York, pp 73–98
- Gorin G, Fiet N, Pacton M (2009) Benthic microbial mats: a possible component to organic matter accumulation in a Lower Aptian oceanic anoxic event. *Terra Nova* 21:21–27
- Hofmann P, Ricken W, Schwark L, Leythaeuser D (2000) Carbon–sulfur–iron relationships and δ¹³C of organic matter for late Albian sedimentary rocks from the North Atlantic Ocean: paleoceanographic implications. *Palaeogeogr Palaeoclimatol Palaeoecol* 163:97–113. doi:10.1016/S0031-0182(00)00147-4
- Holtzapfel T (1985) Les minéraux argileux. Préparation, analyse diffractométrique et détermination, vol 12. Société Géologique du Nord, University of Lille I, Lille, France, p 136
- Jenkyns HC (1999) Mesozoic anoxic events and paleoclimate. *Zentralbl Geol Palaont Teil* 1:943–949
- Karl D, Michaels A, Bergman B, Capone D, Carpenter E, Letelier R, Lipschultz F, Paerl H, Sigman D, Stal L (2002) Dinitrogen fixation in the world’s oceans. *Biogeochemistry* 57:47–98. doi:10.1023/A:1015798105851
- Kenig F, Sinninghe Damsté JS, de Leeuw JW, Hayes JM (1994) Molecular palaeontological evidence for food-web relationships. *Naturwissenschaften* 81:128–130. doi:10.1007/BF01131768
- Konhauser K (2007) Introduction to geomicrobiology. Blackwell, London
- Kuypers MMM, Blokker P, Erbacher J, Kinkel H, Pancost RD, Schouten S, Sinninghe Damsté JS (2001) Massive expansion of marine archaea during a mid-Cretaceous oceanic anoxic event. *Science* 293:92–95. doi:10.1126/science.1058424
- Kuypers MMM, Blokker P, Hopmans EC, Kinkel H, Pancost RD, Schouten S, Sinninghe Damsté JS (2002) Archeal remains dominate marine organic matter from the early Albian oceanic event 1b. *Palaeogeogr Palaeoclimatol Palaeoecol* 185:211–234. doi:10.1016/S0031-0182(02)00301-2
- Lazar B, Eeres J (1992) Carbon geochemistry of marine-derived brines: I. ¹³C depletions due to intense photosynthesis. *Geochim Cosmochim Acta* 56:335–345. doi:10.1016/0016-7037(92)90137-8
- Leuko S, Goh F, Allen MA, Burns BP, Walter MR, Neilan BA (2007) Analysis of intergenic spacer region length polymorphisms to investigate the halophilic archaeal diversity of stromatolites and microbial mats. *Extremophiles* 11:203–210. doi:10.1007/s00792-006-0028-z
- Marsaglia KM (2005) Sedimentology, petrology, and volcanology of the lower Aptian oceanic anoxic event (OAE1a), Shatky Rise,

- North-Central Pacific Ocean. In: Bralower TJ, Premoli Silva I, Malone MJ (eds) Proceedings of the ODP science results, College Station, 198:1–31
- Meyers PA (2006) Paleooceanographic and paleoclimatic similarities between Mediterranean sapropels and Cretaceous black shales. *Palaeogeogr Palaeoclimatol Palaeoecol* 235:305–320. doi:10.1016/j.palaeo.2005.10.025
- Mojzsis SJ, Arrhenius G, McKeegan KD, Harrison TM, Nutman AP, Friend CRL (1996) Evidence for life on Earth before 3,800 million years ago. *Nature* 384:55–59. doi:10.1038/384055a0
- Mustardy L (1996) Development of thylakoid membrane stacking. In: Ort DR, Yocum CF (eds) *Oxygenic photosynthesis: the light reactions*, vol 4. Kluwer, Dordrecht, pp 59–68
- Ohkouchi N, Kashiyama Y, Kuroda J, Ogawa NO, Kitazato H (2006) An importance of diazotrophic cyanobacteria as a primary producer during Cretaceous oceanic anoxic event 2. *Biogeosci Discuss* 3:575–605
- Pacton M, Fiet N, Gorin GE (2007) Bacterial activity and preservation of sedimentary organic matter: the role of exopolymeric substances. *Geomicrobiol J* 25:571–581. doi:10.1080/01490450701672042
- Pacton M, Gorin GE, Fiet N (2008) Unravelling the origin of ultralaminar in sedimentary organic matter: the contribution of bacteria and photosynthetic organisms. *J Sediment Res* 78:654–667. doi:10.2110/jsr.2008.075
- Parkes JR, Cragg BA, Wellsbury P (2000) Recent studies on bacterial populations and processes in subsurface sediments: a review. *Hydrogeol J* 8:11–28. doi:10.1007/PL00010971
- Pedersen TF, Calvert SE (1990) Anoxia vs. productivity: what controls the formation of organic-carbon rich sediments and sedimentary rocks? *Am Assoc Pet Geol Bull* 74:454–466
- Premoli Silva I, Sliter WV (1994) Cretaceous planktonic foraminiferal biostratigraphy and evolutionary trends from the Bottaccione section, Gubbio, Italy. *Palaeontographia Ital* 82:1–89
- Premoli Silva I, Erba E, Salvini G, Locatelli C, Verga D (1999) Biotic changes in Cretaceous oceanic anoxic events of the Tethys. *J Foraminiferal Res* 29:352–370
- Salmon V, Derenne S, Lallier-Vergès E, Largeau C, Beaudoin B (2000) Protection of organic matter by mineral matrix in a Cenomanian black shale. *Org Geochem* 31:463–474. doi:10.1016/S0146-6380(00)00013-9
- Schidlowski M (1988) A 3,800-million-year isotopic record of life from carbon in sedimentary rocks. *Nature* 333:313–318. doi:10.1038/333313a0
- Schidlowski M, Matizgkeit U, Krumbein WE (1984) Superheavy organic carbon from hypersaline microbial mats. *Naturwissenschaften* 71:303–308. doi:10.1007/BF00396613
- Schidlowski M, Gorzawski H, Dor I (1994) Carbon isotopic variations in a solar pond microbial mat: role of environmental gradients as steering variables. *Geochim Cosmochim Acta* 58:2289–2298. doi:10.1016/0016-7037(94)90011-6
- Schlanger SO, Jenkyns HC (1976) Cretaceous oceanic anoxic events: causes and consequences. *Geol Mijnb* 55:179–184
- Schouten S, Hopmans EC, Pancost RD, Sinninghe Damste JS (2000) Widespread occurrence of structurally diverse tetraether membrane lipids: evidence for the ubiquitous presence of low-temperature relatives of hyperthermophiles. *Proc Natl Acad Sci USA* 97:14421–14426. doi:10.1073/pnas.97.26.14421
- Steffen D, Gorin G (1993) Palynofacies of the Upper Tithonian-Berriasian deep-sea carbonates in the Vocontian Trough (SE France). *Bull Cent Rech Explor Prod Elf-Aquitaine* 17:235–247
- Tegelaar EW, de Leeuw JW, Derenne S, Largeau C (1989) A reappraisal of kerogen formation. *Geochim Cosmochim Acta* 53:3103–3106. doi:10.1016/0016-7037(89)90191-9
- Trichet J, Defarge C, Tribble J, Tribble G, Sansone F (2000) Christmas Island lagoonal lakes, models for the deposition of carbonate-evaporite-organic laminated sediments. In: Taberner C, Rouchy JM, Peryt T (eds) *Sedimentary and diagenetic transitions between carbonates and evaporites (special issue)*. *Sediment Geol* 140(1–2):1–8
- Tsikos H, Karakitsios V, Van Breugel Y, Walsworth-Bell B, Bombardiere L, Petrizzo MR, Sinningh  Damst  JS, Schouten S, Erba E, Premoli Silva I, Farrimond P, Tyson RV, Jenkyns HC (2004) Organic-carbon deposition in the Cretaceous of the Ionian Basin, NW Greece: the Paquier Event (OAE1b) revisited. *Geol Mag* 141:401–416. doi:10.1017/S0016756804009409
- Tyson RV (1995) *Sedimentary organic matter: organic facies and palynofacies*. Chapman & Hall, New York
- Weissert H, Lini A, Follmi K, Kuhn O (1998) Correlation of Early Cretaceous carbon isotope stratigraphy and platform drowning events: a possible link? *Palaeogeogr Palaeoclimatol Palaeoecol* 137:189–203. doi:10.1016/S0031-0182(97)00109-0